AEROELASTIC SCALING LAWS WITH CONSIDERATIONS TO THE DESIGN OF AN EXPERIMENTAL SLENDER WING MODEL

E.Cestino*, G.Frulla*, P.Marzocca**
***Department of Aerospace Engineering, Politecnico di Torino, Italy.**
****Department of Mechanical and Aeronuatical Engineering, Clarkson University NY, USA**

Abstract

Innovative aircrafts, such as very long endurance UAVs employ high aspect ratio flexible wings to reduce weight and power in order to achieve sustained flight for months or even years. The increased wing flexibility can lead to large static structural deflections for trimmed flight states. These large deformations can induce aeroelastic instabilities which are quite different from their rigid counterparts. Therefore, it is imperative to perform a flutter analysis which considers the trimmed deflected state as a reference point.

The aeroelastic flutter analysis process should always include an experimental test phase for verification purposes. A wind tunnel test model can provide the opportunity to modify and calibrate theoretical models by showing the effects and the limits of the considered approximations. Two general areas are pertinent to the field of aeroelastic testing. The first includes experiments in which no airstream is present. This class belongs to static and vibrating tests, which are conducted to determine the accuracy of the stiffness distribution, natural frequencies and mode-shapes. The second class includes tests that require the presence of an airstream to study critical and post critical behavior (flutter, LCO amplitude etc.).

An experimental aeroelastic slender wing model can be designed using a scaling procedure. By expressing the aeroelastic equations of motion in dimensionless form, it is possible to relate the behavior of the small scale models to that of a full-scale wing and identify and verify the correctness of those parameters which represent the characteristics of the full-size system and even perform a model updating when required. In this work, a simple numerical method that enables one to expedite the analysis process during the preliminary design phase is introduced. A Typical HALE wing is considered to investigate its aeroelastic behavior and to define a model identification procedure required to develop a wind-tunnel component suitable for experimental test campaigns.

1 Introduction

The objective of this paper is to identify a consistent scaling procedure to investigate the flutter stability problem of a full-size high aspect ratio composite wing structure by means of a laboratory model **[1-5]**.

During the last 50 years dynamically scaled wind tunnel models and scaling considerations – relating wind tunnel test results to the behaviour of a full scale system – have played an important role in aeroelasticity. Such scaling relations relied on dimensional analysis to establish scaling parameters used for scaled models, which are suitable for wind tunnel testing. It is interesting to note that despite its importance, the literature on this topic is not extensive, and most of it was done in the late 1950s and early 1960s (Bisplinghoff et al., 1955; Regier, 1963) **[6-8]**. Similarity methods in engineering dynamics have been discussed by Baker et al. (1991), and the mathematical aspects of scaling and self-similarity has been presented more recently by **[9]**. However, these considerations have only partially been exploited for aeroelastic applications. Often the behaviour of a specific airplane is so complex that the accuracy of theoretical analysis should be verified by experimental tests. Thus model testing becomes necessary to validate theoretical analysis and to perform model updating. By expressing the aeroelastic equations of motion in non-dimensional form or by dimensional analyses, it is possible to indicate a necessary and sufficient set of dimensionless parameters for scaling. Consequenlty, this approach allows a rigorous sensitivity analysis on the characteristic parameters of the model .

Clearly, the use of extremely lightweight structures and the possibility of carrying a considerable amount of non-structural weight, results in a highly flexible aircraft. A proper wing model, which is capable of describing the structural flight deflections should be adopted. In the past few years an approximate nonlinear beam theory which includes terms up to the second order and valid in the range of moderate-to-large deflections (not higher then 10% of the wing span) has been widely accepted **[10,11,12]**. The beam-wise structural model includes the evaluation of the equivalent stiffness for,isotropic configuration and simple thin-walled laminated sections.

Only closed thin-walled sections are considered in this paper with specific laminate lay-up. The introduction of composite material originates a coupling effect in the constitutive equations and the associated displacement field is more complicated than the isotropic counterpart. The beam model considered in the present paper follows a procedure similar to **[13,14]** and is appropriate for a preliminary parametric analysis to evaluate the flutter behaviour of slender wings. For this class of flight vehicles the span-wise dimension can be considered quite higher than transversal section dimensions and the same transversal dimension is higher than the thickness. This is the main reason for the use of a beam model approximation in order to describe the real wing-box and tubular main spar. In this study, the composite box is made of planar and thin plate elements with different lay-ups. Only membrane stresses are accounted for the present developments.

The aeroelastic governing equations are derived in the case of a nonlinear, initially straight and inextensional composite Euler-Bernoulli beam model using the extended Hamilton's principle **[15,16,17]**. The governing partial differential equations of the flexible beam are reduced to a system of ordinary differential equations by using a series discretization technique, along with Galerkin's method, to obtain the aeroelastic governing equations of a simple three degree of freedom system. The unsteady incompressible aerodynamics based on Wagner's function is used to determine the aerodynamic loads based on the strip theory assumption. The aerodynamic model considered in this paper omits the stall model, hence only flutter predictions can be carried out.

A great deal of information about the influence of various system parameters can be obtained by studying the stability of simple models, one of which is introduced in the present article. A Typical HALE wing is considered to investigate the aeroelastic behaviour in undeformed and deformed equilibrium condition. Specific thickness distribution and thin-walled construction are considered for such aircraft structures. The effect of typical parameters, including stiffness ratios, different lay-ups, deflection amplitude, as well as wing aspect ratio, are investigated. Finally a test model further identification procedure is reported. This is based on similarity theory, for the development of an advanced wind-tunnel wing model suitable for an extensive experimental test campaign.

Comparison between analytical and experimental studies are cited from previous experiments **[2,3,4]**, both for the linear and the non-linear studies.

1 Aeroelastic Model

The beam behaviour is described through the longitudinal displacement u(x,t), the transverse displacement v(x,t) and w(x,t), along the y and z axis, respectively, and the torsional angle $\phi(x,t)$ as shown in figure 1. Here X-Y-Z is a global orthogonal coordinate system, while X-s-n is a local coordinate system centred on the mid-line contour of the thin-walled beam section (Fig. 1).

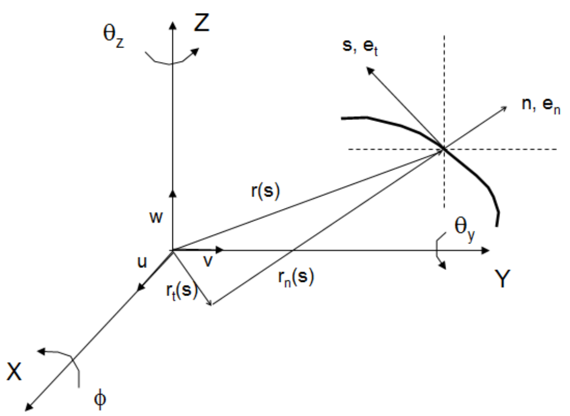

Fig.1. Displacement field for the beam model

A relationship between the two coordinate systems can be established as follows:

$$\vec{r}(s,x) = x\vec{i}_x + y(s)\vec{i}_y + z(s)\vec{i}_z = x\vec{i} + r_n\vec{e}_n + r_t\vec{e}_t \tag{1}$$

In order to transform stresses and strains from the material coordinate system to the X-s-n coordinate system, a simple rotational transformation is used: $\{\sigma\} = [T_\sigma]^{-1}[Q][T_\varepsilon]\{\varepsilon\}$, where $[\bar{Q}] = [T_\sigma]^{-1}[Q][T_\varepsilon]$ and $[T]_\sigma$, $[T]_\varepsilon$ are transformation matrices from local coordinate system to material reference system and Q is the stiffness matrix in the material system for an orthotropic lamina **[18]**.

In the case of slender composite beams it is appropriate to assume that $\sigma_{ss} = \sigma_{nn} = \tau_{sn} = 0$ as indicated in **[15]**. Consequently the reduced stiffness matrix for a single lamina becomes:

$$\begin{Bmatrix} \sigma_{xx} \\ \tau_{xs} \end{Bmatrix}^k = \begin{bmatrix} \tilde{Q}_{11} & \tilde{Q}_{13} \\ \tilde{Q}_{13} & \tilde{Q}_{33} \end{bmatrix}^k \begin{Bmatrix} \varepsilon_{xx} \\ \gamma_{xs} \end{Bmatrix}^k \tag{2}$$

where:

$$\begin{aligned}
\tilde{Q}_{11} &= \frac{\bar{Q}_{13}^2\bar{Q}_{22} - 2\bar{Q}_{12}\bar{Q}_{13}\bar{Q}_{23} + \bar{Q}_{23}^2\bar{Q}_{11} + \bar{Q}_{12}^2\bar{Q}_{33} - \bar{Q}_{11}\bar{Q}_{22}\bar{Q}_{33}}{\bar{Q}_{23}^2 - \bar{Q}_{22}\bar{Q}_{33}} \\
\tilde{Q}_{13} &= \frac{\bar{Q}_{16}\bar{Q}_{23}^2 - \bar{Q}_{13}\bar{Q}_{23}\bar{Q}_{26} - \bar{Q}_{16}\bar{Q}_{22}\bar{Q}_{33} + \bar{Q}_{12}\bar{Q}_{26}\bar{Q}_{33} + \bar{Q}_{13}\bar{Q}_{22}\bar{Q}_{36} - \bar{Q}_{12}\bar{Q}_{23}\bar{Q}_{36}}{\bar{Q}_{23}^2 - \bar{Q}_{22}\bar{Q}_{33}} \\
\tilde{Q}_{33} &= \frac{\bar{Q}_{26}^2\bar{Q}_{33} - 2\bar{Q}_{23}\bar{Q}_{26}\bar{Q}_{36} + \bar{Q}_{36}^2\bar{Q}_{22} + \bar{Q}_{23}^2\bar{Q}_{66} - \bar{Q}_{22}\bar{Q}_{33}\bar{Q}_{66}}{\bar{Q}_{23}^2 - \bar{Q}_{22}\bar{Q}_{33}}
\end{aligned} \tag{3}$$

As an explanatory example, a single-cell, closed cross-section, fiber-reinforced composite thin-walled beam is considered for the advanced aircraft wing modelling. Furthermore, the following assumptions are adopted: the cross-sections do not deform in their own planes; transverse shear effects are discarded (t/2h≤ 0,1 t/2w ≤ 0,1 2w/L ≤ 0,1 2h/L≤0,1); free warping assumption (bi-moment effect discarded), valid for high aspect ratio wing is considered, while hoop stresses are discarded; shear flow is considered constant (Nxs=cost) in the spirit of Batho-Bredt theory; the strains are small and the linear elasticity theory is applied.

Based on these assumptions, the following representation of the 3-D displacement quantities is used where g is a correction function and can be derived as in **[13]:**

$$\begin{aligned}
u &= u_0 - y(s)\vartheta_z + z(s)\vartheta_y - g(s) \\
v &= v_0 - z\vartheta_x \\
w &= w_0 + y\vartheta_x
\end{aligned} \tag{4}$$

where $\vartheta_y = -w_0'$; $\vartheta_z = v_0'$ are introduced according to the Euler-Bernoulli beam approximation.

Assuming that the shear flow is constant, from the condition that the warping function $g(s,x)$ should be a single valued continuous function, it is possible to derive simple analytical solution for the correction function and expression for g **[13,14].** The expression for the stiffness can be derived fromthe constitutive equations in terms of stress resultants by relating the traction F_x, torsional Moment M_x, and bending moments M_y and M_z to the shear flow and axial stress as follows:

$$\begin{aligned}
F_x &= F_1 = \oint\int \sigma_{xx}\,dnds = \oint N_{xx}\,ds \\
M_x &= M_1 = \oint\int \tau_{xs} r_n(s)\,dnds = \oint N_{xs} r_n(s)\,ds \\
M_y &= M_2 = \oint\int \sigma_{xx} z\,dnds = \oint N_{xx} z(s)\,ds \\
M_z &= M_3 = -\oint\int \sigma_{xx} y\,dnds = \oint N_{xx} y(s)\,ds
\end{aligned} \tag{5}$$

The following special cases will be investigated in the present analysis: the isotropic case, that is perfectly uncoupled; the Circumferentially Asymmetric Stiffness (CAS) model that produces bending-twist coupling; and the

[±θ] case that is formally is the same as the isotropic one. The stiffness matrices are respectively:

CASE I ([±θ] configuration):

$$\begin{Bmatrix} F_1 \\ M_1 \\ M_2 \\ M_3 \end{Bmatrix} = \begin{bmatrix} C_{00} & 0 & 0 & 0 \\ 0 & C_{11} & 0 & 0 \\ 0 & 0 & C_{22} & 0 \\ 0 & 0 & 0 & C_{33} \end{bmatrix} \begin{Bmatrix} e \\ \rho_1 \\ \rho_2 \\ \rho_3 \end{Bmatrix} \quad (6)$$

CASE II (CAS configuration):

$$\begin{Bmatrix} F_1 \\ M_1 \\ M_2 \\ M_3 \end{Bmatrix} = \begin{bmatrix} C_{00} & 0 & 0 & 0 \\ 0 & C_{11} & C_{12} & 0 \\ 0 & C_{21} & C_{22} & 0 \\ 0 & 0 & 0 & C_{33} \end{bmatrix} \begin{Bmatrix} e \\ \rho_1 \\ \rho_2 \\ \rho_3 \end{Bmatrix} \quad (7)$$

In absence of warping, the motion of a differential beam element is perfectly described by three translational displacements and three rotations.

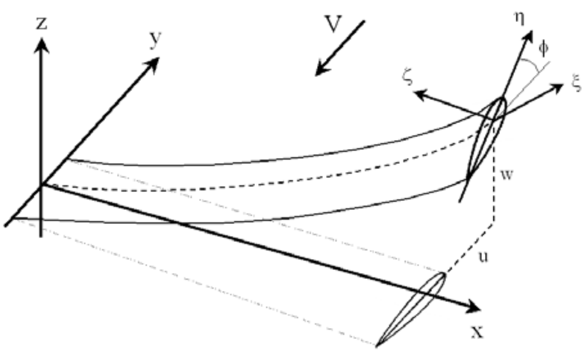

Fig. 2. Deformed and undeformed reference systems

Curvatures respect the 123 axes are defined as $\rho_1 = i_2' \cdot i_3$, $\rho_2 = i_3' \cdot i_1$, $\rho_3 = i_1' \cdot i_2$ where prime indicate first derivative respect to ξ. In the case of a second order approximation the expression of curvatures become:

$$\begin{aligned} \rho_1 &= \phi' + v''w' \\ \rho_2 &= -w'' + v''\phi \\ \rho_3 &= v'' + w''\phi \end{aligned} \quad (8)$$

In the case of a general in-extensional CAS configuration, that is $C_{11} = GJ_t$; $C_{22} = EI_2$; $C_{33} = EI_3$; $C_{12} = K$ the governing equations can be derived according to **[15,16,17]**:

$$\begin{cases} m\ddot{v} + c_2\dot{v} + EI_3 v'''' + \left(EI_3 - EI_2\right)\left(w''\phi\right)'' + \\ +GJ_t\left(\phi' w''\right)' + K\left(\phi''\phi\right)' + K\left(\phi'\phi'\right)' - K\left(w''w''\right)' = q_v \\ m\ddot{w} + c_3\dot{w} + me\ddot{\phi} + EI_2 w'''' - K\phi''' + \left(EI_3 - EI_2\right)\left(v''\phi\right)'' + \\ -GJ_t\left(\phi' v''\right)' - K\left(v'''w'\right)' = q_w \\ j_1\ddot{\phi} + c_4\dot{\phi} + me\ddot{w} - GJ_t\phi'' + Kw''' + \left(EI_3 - EI_2\right)v''w'' + \\ -GJ_t\left(v''w'\right)' + K\left(v'''\phi\right) = q_\phi \end{cases} \quad (9)$$

with the following boundary conditions:

$$\begin{aligned} &v = w = 0,\ \phi = 0,\ w_{,x}, v_{,x} = 0 \text{ at } \xi = 0 \\ &M_1 = M_2 = M_3 = 0,\ V_2 = V_3 = 0 \text{ at } \xi = L \end{aligned} \quad (10)$$

where V_2 and V_3 are the stress resultants along directions 2 and 3 and include nonlinear terms up to second order **[15]**.

The geometrically non-linear structural beam model has been coupled with an unsteady aerodynamic model based on the Wagner indicial function **[7]**. To emphasize the effect of the non-linear structural coupling, when determining the critical aeroelastic condition, only a linear aerodynamic model has been used. Authors are developing a new version of the presented procedure in order to include an unsteady aerodynamic model accounting for stall, useful in analyzing those cases in which the initial angle-of-attack is high. The aerodynamic model considered in this paper omits the stall model, hence only flutter predictions can be carried out. It is assumed that the flight speed is low enough to be well within the incompressible aerodynamics flight speed regime, and the large aspect ratio justifies the use of a 2D strip theory **[7]**. Aerodynamic model is included according to Wagner function approach. Theodorsen function is also applied in conjunction to the FEM developed model. Theodorsen function C(k) and Wagner function $\Phi(t)$ provide the same aerodynamic load representation (but in two different space)at the flutter speed where the oscillations are purely harmonic **[7].**

Expressions for q_v,q_w,q_ϕ are presented in **[2]** and the reader is referred to this for further details. In order to solve the system of governing equations and to study the subcritical and supercritical aeroelastic response as well as the flutter boundaries, the introduction of a small dynamic perturbation about a non-linear static equilibrium is applied. In-plane, out-of-plane, and torsional displacements (v,w,ϕ) are considered as a summation of the static and dynamic components in the undeformed reference system where v_0, w_0, and ϕ_0 are the static in-plane lagging, out-of-plane bending, and torsion displacements due to the aeroelastic trim, (corresponding to a specific flight condition). The problem can be approximated using modal analysis techniques such as:

$$p(x,t) = p_0(x) + \sum_{i=1}^{N_p} f_i(x)\, p_i(t) \qquad (11)$$

where p assumes the meaning of generic displacement (v,w,ϕ) **[2,3,4],** and f_i are mode shapes derived from a vibrating, non-rotating uniform cantilever beam according to :

$$\begin{aligned} f_{v,w} &= \cosh(\alpha_i L\hat{x}) - \cos(\alpha_i L\hat{x}) - \beta_i\left[\sinh(\alpha_i L\hat{x}) - \sin(\alpha_i L\hat{x})\right] \\ f_\phi &= \sqrt{2}\sin(\gamma_i L\hat{x}) \end{aligned} \qquad (12)$$

where $\alpha_i, \beta_i, \gamma_i$ depend on the number of mode considered, the tip store moment of inertia about wing elastic axis, I_ϕ, and the mass of tip store, M. In the case of a single mode approximation without tip mass $\alpha_i L$= 1,875 β_i= 0,734 $\gamma_i L$=1,57. Finally, it is possible to identify two aeroelastic governing systems: (1) a static aeroelastic non-linear equilibrium system, and (2) a dynamic perturbed system, reduced to its linear approximation in the dynamic components **[2,3,4,5].** The use of a simplified model is justified, especially in the preliminary design phase where analytical methods are preferred with respect to complex commercial FEM models. It is worth remarking that FEM models are capable of dealing with selected aspects needed for the non-linear aeroelastic design, but not without complex model updating which might become cumbersome in preliminary design activities.

The simple case derived in this paper (SM model) is obtained reducing the problem to a 3 DOFs by using a “single mode” approximation. Applying Galerkin’s condition to the residuals, a set of ordinary equations is obtained from the original PDEs system. The resultant derived equivalent stiffness will permit a very good correlation in terms of frequencies of first lagging, flapping, and torsional modes. A discrete level of correlation exists in static terms and the correlation can be improved increasing number of modes. The state-space form of the unsteady aerodynamic formulation makes it particularly suitable for upcoming control studies. Consequently, introducing a state vector X, the final state-space system can be cast as:

$$\{\dot{X}\} = \left[A\left(\Gamma, \Theta, \bar{K}, \bar{X}_\alpha, \bar{r}_\alpha, k, \mu, \mu_M, I_M, \lambda, a, v_0, w_0, \phi_0\right)\right]\{X\} \qquad (13)$$

The equation 15 is function of 12 dimensionless parameters because v_0, w_0, ϕ_0 are all dependant to α_{root} and their definition is reported in the following section.

The matrix [A] contains linear terms of the perturbed system function of the equilibrium solution. The stability about the equilibrium operating condition is determined by the eigenvalue behavior of [A] matrix. The eigenvalues extraction is performed by means of a MATLAB code. Linear flutter speed (LFS) can be computed assuming the equilibrium static configuration as zero. By including such equilibrium terms, a non-linear flutter speed (NLFS) analysis can be performed.

2 Aeroelastic parameters

By expressing the aeroelastic governing equations in dimensional or dimensionless form, it is possible to relate the behaviour of the small scale models, to that of full-scale aircraft. The Buckingham π theorem is the central result of dimensional analysis and provides a method for computing sets of dimensionless parameters from the given variables even if the form of the equation is still unknown. However, the choice of dimensionless parameters is not unique: Buckingham's theorem only provides a way of generating sets of dimensionless parameters, not the most 'physically meaningful'. Buckingham's theorem allows to conclude that the equation can be expressed in the form of a relationship among p=n-m dimensionless products (Π), in which p=n-m is the number of products in a complete set of products of the variables n and m is the number of fundamental dimensions. The main gain is the reduction of the number of variables from n to n-m. Similarity is guaranteed by the equalities of $\Pi_i = \Pi_i^*$, $(i = 1,2,\ldots(n-m))$, where Π_i and Π_i^* are values of Π_i when real and experimental variables are introduced, respectively. It is possible to observe that if the system is composed by r equations as:

$$\begin{cases} \Pi_1 = \varphi_1'\left(\Pi_{r+1},\ldots\Pi_{n-m}\right), \\ \ddots \\ \Pi_r = \varphi_r'\left(\Pi_{r+1},\ldots\Pi_{n-m}\right), \end{cases} \tag{14}$$

It is sufficient to maintain the equality from true and scaled models of $n-r-m$ parameters $\Pi_{r+1},\ldots,\Pi_{r-m}$ in order to have the similarity because the equality of $\Pi_1,\ldots,\Pi_r$ is automatically obtained by equations (14).

The number of dimensionless products related to the case of an advanced high aspect ratio wing is increased with respect to the linear counterpart. It is possible to highlight the following 25 parameters and 3 fundamental dimensions (M,L,T): v, w, ϕ (lag, flap, and torsional displacements), α_{root} (root static angle of attack), b (semichord), L(semispan), EI_3, EI_2, GJ, K, (bending, torsion and coupling stiffness) V_∞ (airspeed), m (wing mass per unit length), M (tip mass), I_ϕ (tip store moment of inertia), e (section mass center from elastic axis), r_α (radius of inertia), ρ (air density), a (dimensionless elastic axis location), v_0, w_0, ϕ_0 (lag, flap, and torsional static Displacements), $W_{1,2,3,4}$ (Wagner states). The mathematical model is composed by 3 dynamic perturbed equations, 3 static equilibrium equations and 4 lag equation, in the case of Wagner aerodynamic approach, so we obtain p=25-3-6-4=12 The following dimensionless parameters has been considered:

$$\begin{aligned} &\alpha_{root}; k^* = \frac{\omega_r \cdot b}{U}; \lambda = \frac{L}{b}; \mu = \frac{m}{\pi\rho b^2}; \mu_M = \frac{M}{mL}; \\ &I_M = \frac{I_\phi}{mr^2 L}; \Gamma = \frac{EI_3}{EI_2}; \bar{K} = \frac{K}{GJ_t}; \Theta = \frac{EI_2}{GJ_t}; \\ &\bar{X}_\alpha = \frac{e}{b}; \bar{r}_\alpha = \frac{r_\alpha}{b}; a \end{aligned} \tag{15}$$

By using these dimensionless similarity parameters the aeroelastic governing equations can be re-written as

$$\begin{cases} \ddot{v} + \frac{\Gamma\Theta\bar{r}_\alpha^2}{\lambda^2} v'''' + \frac{\Gamma\Theta\bar{r}_\alpha^2}{\lambda^2}(\Gamma-1)\left(w''\phi\right)'' + \frac{\bar{r}_\alpha^2}{\lambda^2}\left(\phi' w''\right)' + \\ \frac{\bar{K}}{\lambda}\bar{r}_\alpha^2\left(\phi''\phi\right)' + \frac{\bar{K}}{\lambda}\bar{r}_\alpha^2\left(\phi'\phi'\right)' - \frac{\bar{K}}{\lambda^3}\bar{r}_\alpha^2\left(w''w''\right)' = \hat{L}_v \\ \ddot{w} + \bar{X}_\alpha\ddot{\phi} + \frac{\Theta\bar{r}_\alpha^2}{\lambda^2} w'''' - \frac{\bar{K}}{\lambda}\bar{r}_\alpha^2\phi''' + \frac{\Gamma\Theta\bar{r}_\alpha^2}{\lambda^2}(\Gamma-1)\left(v''\phi\right)'' + \\ -\frac{\bar{r}_\alpha^2}{\lambda^2}\left(\phi' v''\right)' - \frac{\bar{K}}{\lambda^3}\bar{r}_\alpha^2\left(v'''w'\right)' = \hat{L}_w \\ \bar{r}_\alpha^2\ddot{\phi} + \bar{X}_\alpha\ddot{w} - \bar{r}_\alpha^2\phi'' + \frac{\bar{K}}{\lambda}\bar{r}_\alpha^2 w''' + \frac{\Gamma\Theta\bar{r}_\alpha^2}{\lambda^2}(\Gamma-1)v''w'' + \\ -\frac{\bar{r}_\alpha^2}{\lambda^2}\left(v''w'\right)' + \frac{\bar{K}}{\lambda}\bar{r}_\alpha^2\left(v'''\phi\right) = \hat{M}_\phi \end{cases} \tag{16}$$

where the aerodynamic load components $\hat{L}_v, \hat{L}_w, \hat{M}_\phi$ are functions of μ, k^*, a. When in-plane, out-of-plane, and torsional displacements (v,w,ϕ) are considered as a summation of the static and dynamic components in the undeformed reference system (v0, w0, and ϕ0 are the static in-plane lagging, out-of-plane bending, and torsion displacements and are all dependant to α_{root}), the dimensionless parameter α_{root} should be also included while the tip-mass parameters μ_M, I_M are already considered as in eq. (12).

3 Scaling of a typical HALE wing

In order to illustrate the application of the scaling procedure and flutter model theory developed in the previous section, the flutter computation of a typical high aspect ratio HALE wing flying at an altitude of 20 km is considered. The HALE geometry is presented in figure 3 and correspondent dimensionless parameters are reported in Table 1. The wing structure is based on a structural configuration with an in-plane, out-of-plane and torsional stiffness of $EI_3 = 1.9\text{E+06 Nm}^2$, $EI_2 = 5.00\text{E+04 Nm}^2$ $GJ = 5{,}11\text{E+04 Nm}^2$ respectively. The wing total mass is about 43.2 kg. Span-wise elastic axis and CG location are both positioned at 50% of the local chord c that is 1.41 m. The mass moment of inertia is about 0.224 kg·m.

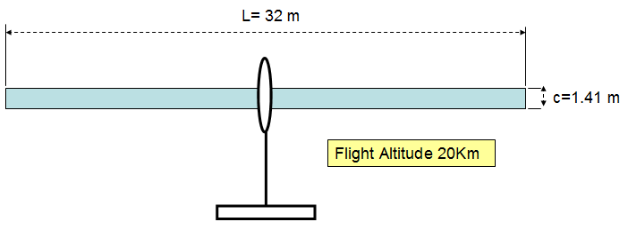

Fig. 3. Typical HALE Model

Table 1

k*	μ	Θ	Γ	X_α	r_α	A	λ	α	K
-	10,8	0,98	38	0	0,6	0	22,7	3°	0

The case of a wind-tunnel model where compressibility, and thus Mach number as well Reynolds number, is presumed to have no effect is considered. It is important to note that the Reynolds number of the model test in the wind tunnel will usually be less than that of the wing at flight altitude. For the considered case the model Re # is about 100.000, while the aircraft Re # is about 400.000. However the effect of changes of Reynolds number on the aerodynamic loads is relatively small, at least in a first approximation case, and values of flutter speed as well flutter frequency are less sensitive to Reynolds number variations **[7]**. Clarkson University subsonic wind-tunnel (Figure 8) has a test section of 1.22 m wide by 0.91 m tall with a length of 1.67 m. Considering the wind tunnel test section a geometrical scale ratio for a model wing of about $L_m/L_v \sim 1/30$ has been adopted.

Wing models will be mounted, through a variable angle-of-attack support, vertically into the wind-tunnel, to overcome the effect of the load due to gravity. The theoretical flutter speed (both LFS "flutter velocity in linear equilibrium condition" and NLFS "flutter velocity in non-linear equilibrium condition") will be lower than maximum speed obtainable in the tunnel that is approximately 70 m/s. Because the length ratio has been defined and the same aspect ratio should be obtained, the model semi-chord is derived and in particular b = 23 mm was selected. Because the mass ratio μ should be the same it is possible to obtain the model mass ratio as:

$$\frac{m_m}{m_w} = \frac{\left(\pi\rho b^2\right)_m}{\left(\pi\rho b^2\right)_w} = \frac{\rho_m b_m{}^2}{\rho_w b_w{}^2} \Rightarrow \frac{m_m}{m_v} \sim \frac{1}{61} \qquad (17)$$

Remembering that the wing properties in this example do not vary along the span, the bending stiffness of the model will be:

$$\frac{\left(EI_2\right)_m}{\left(EI_2\right)_v} = \frac{\left(EI_3\right)_m}{\left(EI_3\right)_v} = \frac{\left(GJ\right)_m}{\left(GJ\right)_v} \sim \frac{1}{150000} \qquad (18)$$

The LFS computation can be performed assuming the equilibrium static configuration as zero, that is wtip/b=0.

The NLFS calculation with the SM approximation for both the tunnel model scale and the real full scale wing was performed and a ratio of NFS/LFS=0.45 was obtained.

For both cases the static values are about w_0/b=2,39 and ϕ_0=0,0114 at the flutter speed .

The first natural frequencies in vacuum and the critical reduced frequency for the two cases are reported in table 2. These cases demonstrate a similar behaviour both in non-dimensional frequency and in damping, assessing the consistency of the developed similarity procedure.

Table 2

Linear	ω_1 [Hz] (flap)	ω_2 [Hz] (lag)	ω_3 [Hz] (tors)	k*
Typical HALE	0,42	2,59	7,46	0,359
Scaled Model	8,04	49,59	142,44	0,359
Non Linear	**ω_1 [Hz] (coupled)**	**ω_2 [Hz] (coupled)**	**ω_3 [Hz] (coupled)**	
Typical HALE	0,42	2,35	7,54	0,78
Scaled Model	8,03	44,88	143,99	0,78

4 Advanced composite wind tunnel model

An advanced experimental model is proposed and will allow to study different aeroelastic phenomena with the same low cost model, developing a modular concept that provide the opportunity to modify and calibrate the test practices to account for non-linear structural responses and other non conventional phenomena. A first generation of this model is a rectangular wing, untwisted, and flexible in flap, lag, and torsion.

A wing with symmetric NACA airfoil sections and composed by pieces of resin supported by a composite fiber box was selected. Resin parts are only bonded to the main spar leaving micro-gaps between the resin parts in order to reduce torsional stiffness. The span is about 520 mm, chord 46 mm and the uniform mass per unit length of the overall wing (aerodynamic and structural elements) is about 0.0219 kg/m. A slender body at the wing tip is designed to provide enough torsional inertia in order to induce flutter in the velocity range of the wind tunnel **[1,2,5]**. Different aspect ratio wings and different layup solutions (uncoupled configurations or CAS) can be tested by simply replacing the composite spar and suitably redistributing the aerodynamic sections. An example of the technology applied is shown in Figure 4, along with a detail of the wind tunnel link and the area of wing tip with the possibility to use different tip solutions to meet the wind tunnel speed limits. In order to create a virtual test, the analytical solution is compared with a QUAD4 FEM model simulating the thin-box structure. The simplified beam-like model, as presented in previous section, and the FEM wing-box structure model has been used to asses the static and dynamic behaviour of a composite rectangular closed cross-section with different ply angles orientation.

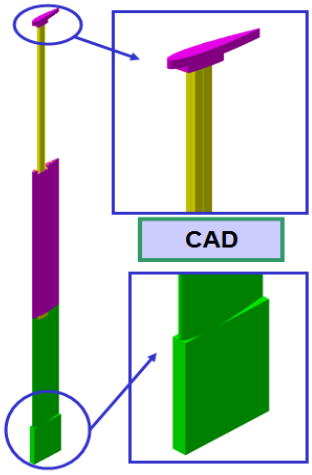

Fig. 4. Advanced Wind Tunnel Model

The geometry of the rectangular wing-box structure is maintained constant for all the analyzed cases as well as the stacking sequence of the left (side 3) and right (side 1) sides and mass properties. Only the initial lay-up of each top (side 2) and bottom (side 4) sides are changed in order to obtain different combinations of structural dimensionless parameters as in figure 5.

Lay-up	Γ	$\bar{K}$	Θ
0	26,84	0,00	8,37
10	21,59	1,20	4,44
20	22,67	0,91	1,73
30	34,32	0,56	0,81
40	54,30	0,29	0,52

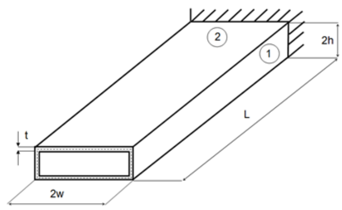

Fig. 5: Wing box section and dimensionless parameters

Static assessment of stiffness dimensionless parameters is performed starting from the inverse of eq. (6) (CAS):
Applying firstly a unitary force in z direction which produces a moment $M_y = 1 \cdot (x - L)$ and then a unit torque $M_x = 1$ it is possible to numerically derive the following dimensionless

parameters having calculated the respective curvatures:

$$\overline{K}_{FEM} = \frac{(\rho_y)_{M_x=1}}{(\rho_y)_{F_z=1}} \; ; \; \Theta_{FEM} = \frac{(\rho_x)_{M_x=1}}{(\rho_y)_{F_z=1}} \tag{19}$$

Applying a unitary force in y direction, the parameter Γ can be derived by the following relation:

$$\Gamma_{FEM} = \left[1 - \frac{\overline{K}^2}{\Theta}\right] \frac{(\rho_y)_{F_z=1}}{(\rho_z)_{F_y=1}} \tag{20}$$

Figure 6 shows the comparison between theoretical stiffness parameters used in the simplified model and coefficients derived from the virtual test (wing box FEM model). This assessment shows a good correlation between the beam-like model and the FEM model.

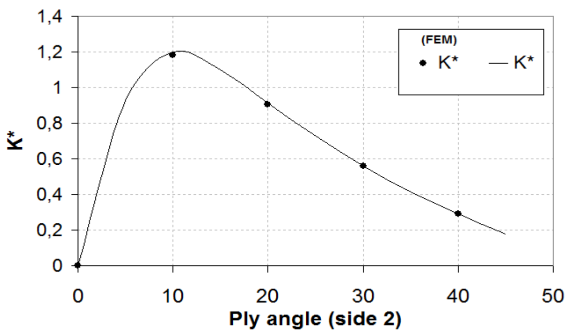

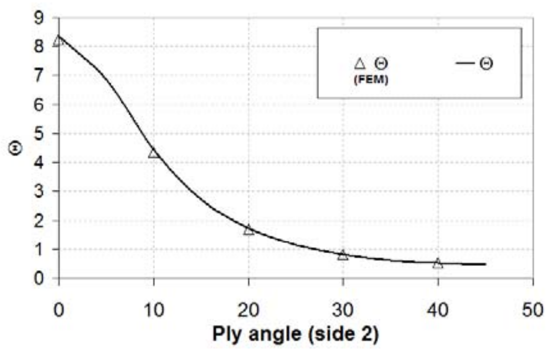

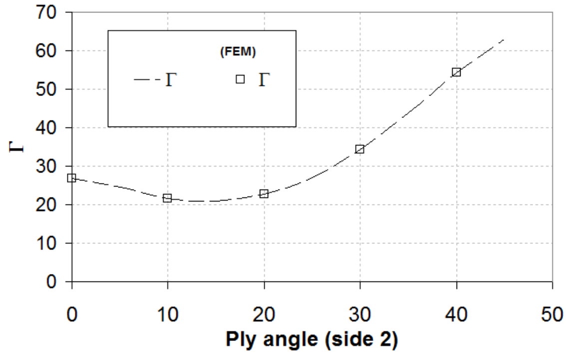

Fig. 6. Analytical and FEM stiffness assessment

A dynamic assessment has been carried out considering the first three modes in the analytical model and the first five structural modes in the FEM model. The dynamic assessment presents a very good correlation in terms of frequency and mode shapes of the first coupled flap/torsion and first torsion/flap modes, and uncoupled first lag mode. In the case of FEM modes 1, 5 and 3 are first coupled flap/torsion and first torsion/flap modes and uncoupled first lag mode respectively. Modes 2 and 4 are then second and third flap/torsion modes. Comparison of correspondent frequency is reported in figure 7.

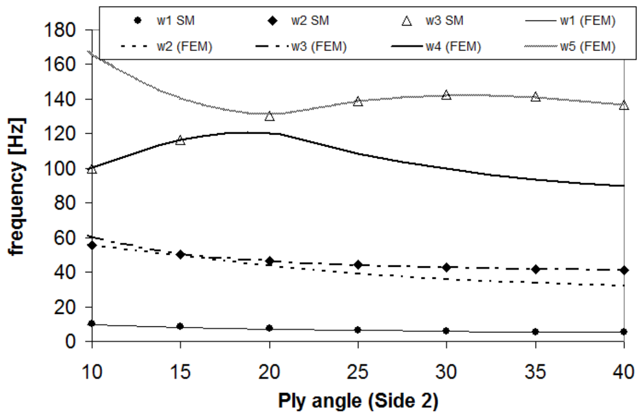

Fig. 7. Analytical and FEM frequency comparison

In the case of 10° ply angle, the first FEM flap/torsion, torsion/flap, and lag modes change the order and become mode 1, 4, and 2 as indicated in figure 7. It is possible to conclude that even with the SM approximation, the first flap/torsion, first torsion/flap, and uncoupled first lag mode are well approximated by the SM analytical model.

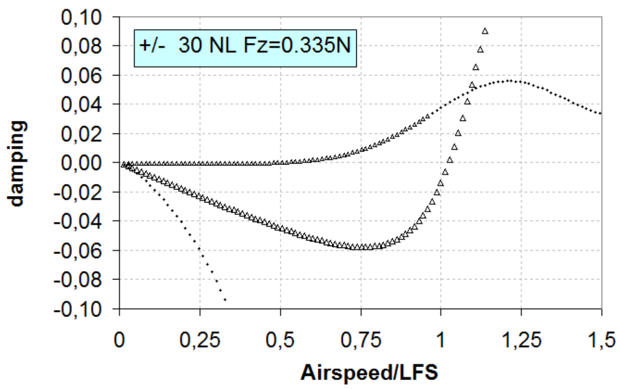

Fig. 8. SM damping results in the linear case and with an imposed vertical force Fz=0.335N

In order to introduce specific behavior typical of long slender composite wings, the basic configuration ($[\pm 30]$ layup) has been modified introducing the vertical deflection and rotation due to a force in z direction that produce in the beam-like model an equal static deflection ratio w/L=0.1. When the wing deforms under loading, its dynamics reveals a non-linear coupling between torsion and lagging bending also when the composite coupling stiffness (K) is equal to zero as in the case shown in figure 8. Thus, the flutter characteristic of a deflected wing is different from those where the undeformed configuration remains virtually unchanged. The inclusion of structural geometric non-linearity is the basis for the determination of such a non-conventional aspect **[12,5]**. Damping characteristic is shown in Figure 8 as function of airspeed. The nonlinear result is obtained with an imposed vertical force Fz=0.335N. A comparison to FEM approach based on a nonlinear static FEM solution and Theodorsen's function approximation is also performed considering the same vertical force. Results are included in table 3.

Table 3

	NLFS/LFS
SM Analytical	0,47
FEM Approach	0,53

It is possible to observe a ratio of NLFS/LFS (SM)=0.47 in the case of a single mode approximation and NLFS/LFS (FEM)=0.53 in the case of a FEM approach. FEM approach demonstrates a slightly higher deflection with respect to SM solution. This is expected from the simplifications have been made.

4 Preliminary balsa wind tunnel tests

The experimental activity has been initiated in order to validate the theoretical model previously described. At present, only a few test cases of typical slender wing configurations, whose geometrical and structural characteristics are consistent with the model assumptions, were studied and cited from previous experimental tests **[2,3,5]**. These experiments are certainly not sufficient for a complete verification of the wing behaviour; however, the correlation with the model was quite satisfactory. Preliminary experimental study has been conducted on a balsa wing model and main characteristics in terms of dimensionless parameters are reported in Table 4.

Table 4

μ	Θ	Γ	X_α	r_α	a	λ	w_{tip}/b
10,8	0,98	96	0	0,578	0	22,7	2,82

In all the experiments a magnetic sensor, Vernier MB-BTA (200 samples per second), was used to record the variation in magnetic field produced by a 'rare-heart magnet' (low mass and high magnetic field) attached to the wing tip figure 9.

The magnetic field is correlated with the displacement, and it was possible to record the tip displacement during the experimental campaign. Multiple tests were conducted at different speeds and angles-of-attack.

The flutter characteristics obtained from the experiments are compared with the numerical simulations based on the theoretical model. A good correlation between these results are clearly present.

Fig. 8. preliminary wind tunnel tests

In addition, consistent with reference **[1]**, a hysteresis behaviour was found during the test of loading and unloading of the wing in the proximity of the flutter speed, confirming that these highly flexible wings exhibit a subcritical Hopf bifurcation, implying that a stable limit cycle oscillation (LCO) occurs above the NLFS. This LCO remains stable and its amplitude increases as the speed increases **[1,3]**. This hysteresis was not observed in the numerical investigations, and this could be due to the fact that stall and flow separation, as well as structural damping **[1]**, have not been included in the present model.

Table 5

	NLFS/LFS
SM Analytical	0,430
Experimental UP	0,592
Experimental DOWN	0,566

Experimental tests show a flutter speed ratio of NLFS/LFS = 0.592 in the increasing velocity phase (Exp Flutter UP) and a flutter speed of about NLFS/LFS = 0.566 (Exp Flutter DOWN) in the decreasing velocity phase. A static deflection of approximately 63-65mm was recorded at the flutter speed. With the aforementioned analytical analysis (using the simplified model SM), and setting α_{root} to reproduce the experimental value of the static tip deflection, a theoretical NLFS ratio of approximately NFS/LFS = 0.43 was obtained. This confirms the different flutter behaviour characteristic of an highly flexible flying wing and the validity of a simplified model for the subsequent preliminary flutter evaluation. This is valid for both the linear and nonlinear cases (Table 5). More experiments will be conducted on an advanced composite model in order to show potential advantages coming from changes in the lamination angle of a box-beam plates model, in the linear and nonlinear cases. The effect of addition of a tip mass on the critical flutter condition will also be investigated.

5 Conclusions

A composite thin-walled nonlinear beam model has been used for the study of the aeroelastic stability of high aspect ratio wings in an incompressible flow. To this end a simplified analytical method capable of expediting the calculation process during the preliminary design phase has been developed by means of a single mode Galerkin approximation. Preliminary results have been compared with FEM analysis in order to assess the accuracy of the prediction. The SM model demonstrated a satisfactory static and dynamic behavior confirming its validity for the subsequent preliminary flutter evaluation both in the linear and nonlinear cases. The introduction of a CAS composite box produces a coupling effect both in frequency and in mode shape, also in the linear flutter case where the nonlinear equilibrium parameters are not present. When the effect of the deflected equilibrium configuration is considered, the system reveals a non-linear coupling between torsion and lagging bending even when the composite coupling stiffness is equal to zero. A test model identification procedure, based on similarity theory, is also reported in order to study the flutter aeroelastic stability problem of a full-size high aspect ratio wing structure. For such purpose a wind tunnel laboratory model is introduced as a useful mean for the investigation and verification of analytical theoretical prediction. Analytical and experimental comparisons are cited from previous experiments showing the good prediction of the presented simplified analytical model.

References

[1] Tang, D., Dowell, E.H., "Experimental and Theoretical Study on Aeroelastic Response of High-Aspect-Ratio Wings," AIAA Journal, Vol. 39, No. 8, pp. 419-429, 2001.
[2] Cestino, E., "Design of very long-endurance solar powered UAV," PhD Dissertation Politecnico di Torino, Aerospace Dept. , Torino, 2006.
[3] Romeo, G., Frulla, G., Cestino, E., Marzocca, P., Tuzcu, I. "Nonlinear Aeroelastic Modelling and Experiments of Flexible Wings," Proc. of 47th AIAA/ASME/ASCE/AHS/ASC Structures, Structural Dynamics, Materials Conference, Newport RI, 1-4 May, 2006.
[4] Frulla G., Cestino E. "Preliminary design of aeroelastic experimental slender wing model" AIRTEC2009 Int. Conf. (Frankfurt - Germany) 3-5 November 2009.
[5] G. Frulla, E. Cestino, P. Marzocca "Critical behaviour of slender wing configurations" Proc. of the institution of mechanical engineers. Part G, Journal of Aerospace Engineering Vol.224 pp.527-636 2010.
[6] P.P. Friedmann, Aeroelastic scaling for rotary-wing aircraft with applications, Journal of Fluids and Structures 19 (2004) 635–650.
[7] Bispringhoff, R., Ashley, H., and Halfman, R. Aeroelasticity,1955 (Dover, New York).
[8] Baker, W.E., Westine, P.S., Dodge, F.T., 1991. Similarity Methods in Engineering Dynamics: Theory and Practice of Scale Modeling, Revised Edition. Elsevier, Amsterdam.
[9] Barenblatt, G.I., 1996. Scaling, Self-similarity, and Intermediate Asymptotics. Cambridge University Press, Cambridge.
[10] Friedmann, P.P., Glaz, B., Palacios, R. A moderate deflection composite helicopter rotor blade model with an improved cross-sectional analysis. International Journal of Solids and Structures, 2009, 46 (10) ,2186–2200.
[11] Antona E., Frulla G., "Some considerations about the concepts of asymptotic approach". Atti dell'Accademia delle Scienze di Torino, 135,pp. 135-161,2001.
[12] Frulla, G. "Aeroelastic Behavior of a Solar-Powered High-Altitude Long Endurance Unmanned Air Vehicle (HALE-UAV) Slender Wing" Journal of Aerospace Engineering, Vol. 218, Part G, Special Issue 2004.
[13] Berdichevsky V., Armanios E.A.,Badir, A.M. "Theory of Anisotropic Thin-Walled closed-cross-section Beams". Composites Engineering. Vol. 2, no.5-7, 1992, pp.411-432.
[14] Armanios E.A., Badir, A.M. "Free Vibration Analysis of Anisotropic Thin-walled Closed-Section Beams" . AIAA Journal Vol. 33, No. 10, October 1995. pp. 1905-1910.
[15] Nayfeh, A.H., Pai, P.F. Linear and Non-linear Structural Mechanics, 2004 (Wiley Interscience, New York).
[16] Hodges, D.H., Dowell, E.H. Nonlinear Equations of Motion for the Elastic Bending and Torsion of Twisted Non Uniform Rotor Blades, NASA TN D-7818, 1974.
[17] Crespo da Silva, M.R.M., Glynn, C.C. Nonlinear Flexural-Flexural-Torsional Dynamics of Inextensional Beams. Equations of Motion. Journal of Structural Mechanics, 1978, 6(4), 437-448.
[18] Cestino E., Frulla G.: "Critical Aeroelastic Behaviour of slender composite wings in an incompressible flow" *Composite Materials in Engineering Structures* NOVA Publisher 2010, in press..

Copyright Statement